Geotechnical and Geophysical Site Characterisation 5 – Lehane, Acosta-Martínez & Kelly (Eds)
© 2016 Australian Geomechanics Society, Sydney, Australia, ISBN 978-0-9946261-2-7

Empirical estimation of soil unit weight and undrained shear strength from shear wave velocity measurements

S.W. Moon & T. Ku
Department of Civil and Environmental Engineering, National University of Singapore, Singapore

ABSTRACT: The main objective of this study is to establish useful empirical relationships to estimate engineering properties of soil in terms of geotechnical applications of shear wave velocity (V_s). Based on each special database compiled from globally well-documented geotechnical test sites, site-specific stress-normalized V_s and downhole-type shear wave mode are utilized for estimating soil unit weight and undrained shear strength, respectively. In addition, the application of proposed global empirical relationships is examined at two test sites (i.e., Australia and China) as independent case studies. The geological setting and geotechnical characterization of the two test sites are summarized and further discussions are described in detail. Using the proposed correlations, it is shown that field shear wave velocity measurements can offer reasonable profiles of the soil unit weight and undrained shear strength at given sites.

1 INTRODUCTION

Shear wave velocity (V_s) of geo-materials such as soils and rocks is one of the fundamental engineering measurements for geotechnical design problems due to its direct relationship with initial shear modulus (G_0) at small strains. Indicating the beginning of all stress-strain-strength curves, the initial shear modulus is calculated using $G_0 = \rho \cdot V_s{}^2$, where ρ is the bulk soil density. It is employed for performing site response analysis as well as ground deformation analysis with respect to foundation system.

For measuring shear wave velocity, borehole seismic methods (downhole test or crosshole test) and non-invasive geophysical techniques (surface wave survey or reflection test/refraction test) as well as laboratory testing methods (bender element test or resonant column test) have been developed. The utilization of in-situ V_s data for establishing several empirical relationships may lead to potential uncertainty coupled with scattered outliers attributed to inherent site conditions and sensitivity of applied test methods. Nevertheless, in-situ V_s measurement techniques are generally efficient and suitable for assessment of geotechnical engineering problems since V_s data can be obtained quickly and economically with minimum soil disturbance. Furthermore, G_0 calculated from in-situ V_s measurement is commonly considered to be more accurate and reliable than that determined from laboratory tests, which generally present lower G_0 due to sample disturbance, stress relief, and loss of ageing effect (Ghionna and Jamiolkowski 1991; Ku and Mayne 2014; Stokoe and Santamarina 2000; Tatsuoka and Shibuya 1992).

In several previous studies, the in-situ V_s measurements have been applied to establish empirical correlations with engineering properties of soils (e.g., soil unit weight, γ_t; peak friction angle, ϕ_p; and undrained shear strength, s_u) (Levesques et al. 2007a; Mayne 2007b; Uzielli et al. 2013). Using two special databases compiled worldwide, this paper describes two new global empirical relationships between: (1) soil unit weights (γ_t) and in-situ site-specific stress-normalized shear wave velocity, instead of conventional $V_s - \gamma_t$ models; (2) undrained shear strength (s_u) and shear wave velocity.

2 PROPOSED RELATIONSHIPS

2.1 *Normalized shear wave velocity – unit weight*

For this study, a special database (Mayne et al. 2009) is applied based on 120 well-documented test sites consisting of 61 clay sites, 6 fissured and calcareous sites, 8 silt sites, 35 sand sites, and 10 other sites. The ranges of compiled engineering properties of soils such as plasticity index (PI), void ratio (e), and total unit weight (γ_t) are summarized in Table 1.

For assessment of seismic liquefaction potential of soils, the in-situ measurements of V_s have been normalized by effective overburden pressure (σ'_{v0}) adopting a constant exponent of 0.25 at the reference

Table 1. Details of collected database: soil type, number of site and data, and range of soil properties (PI, e, γ_t, V_{s1}, V_{sn}) used for correlation between unit weight and normalized shear wave velocity (data from Mayne *et al.* 2009).

Soil Type	No. of Site	No. of Data	Range of PI	Range of e	Range of γ_t (kN/m^3)	Range of V_{s1} (m/s)	Range of V_{sn} (m/s)	Symbol
Intact Clay	61	698	0-250	0.40-6.75	11.2-22.7	35-406	39-438	
Fissured Clay	3	21	12-55	0.43-0.84	18.8-21.3	178-313	187-306	
Calcareous Clay	3	18	0-11	0.95-1.38	16.2-19.7	186-400	182-535	
Silts	8	32	0-15	0.64-1.43	16.7-20.2	122-319	142-215	
Sands	35	200	0-11	0.43-2.15	14.9-22.2	106-621	88-728	
Gravels	7	43	-	0.27-0.70	19.6-22.5	120-366	263-280	
Clay Till	3	16	0-11	0.19-0.56	20.1-24.0	188-611	242-645	

stress of 1 atmospheric pressure (Kayen et al. 2013). On the other hand, a site-specific exponent that depends on actual geostatic stress condition at each site can be employed for the normalization of V_s instead of the constant exponent 0.25. In this study, stress-normalized shear wave velocity (V_{s1}) and site-specific stress-normalized shear wave velocity (V_{sn}) of various geo-materials are calculated from the following equations, respectively:

$$V_{s1} = V_s\,(m/s) / (\sigma'_{v0} / \sigma_{atm})^{0.25} \quad (1)$$
$$V_{sn} = V_s\,(m/s) / (\sigma'_{v0} / \sigma_{atm})^{n} \quad (2)$$

where σ'_{v0} = effective overburden pressure, σ_{atm} = 1 bar = 101.325 kPa = atmospheric pressure, n = site-specific stress exponent. As noted in Equation 1, the exponent 0.25 has been commonly determined as an empirical value based on laboratory tests with clean silica sands (Stokoe et al. 1985; Yu and Richart 1984). However, the exponent n in Equation 2 can be estimated to have various values because it is often significantly dependent on the site-specific conditions as noted by Ku *et al*. (2011).

In order to obtain better fitting models, involving an increase in coefficient of determination (R^2) and decrease in the standard error of the dependent variable (S.E.Y.), higher order regressions are examined using stress-normalized V_s and PI. Two empirical correlations for the estimation of total unit weight are observed in Figure 1 as a function of both PI and V_{s1} or V_{sn}:

$$\gamma_t = 11.27(V_{s1})^{0.147}(PI)^{-0.096} \quad (3)$$
$$\gamma_t = 7.91(V_{sn})^{0.194}(PI)^{-0.068} \quad (4)$$

As described in Figure 1, Equation 3 and 4 present improved γ_t relationships for clay and clay tills from the database collected. In addition, the proposed expression (N = 39; R^2 = 0.768; S.E.Y. = 0.069) using V_{sn}, Equation 4, is comparable with that (N = 53; R^2 = 0.726; S.E.Y. = 0.074) using V_{s1}, Equation 3. Based on the observed statistical information, the regression model using V_{sn} can be considered to be slightly more robust. Apparently, both normalized shear wave velocities are proven to have strong relationships with soil unit weight in spite of some scattered data.

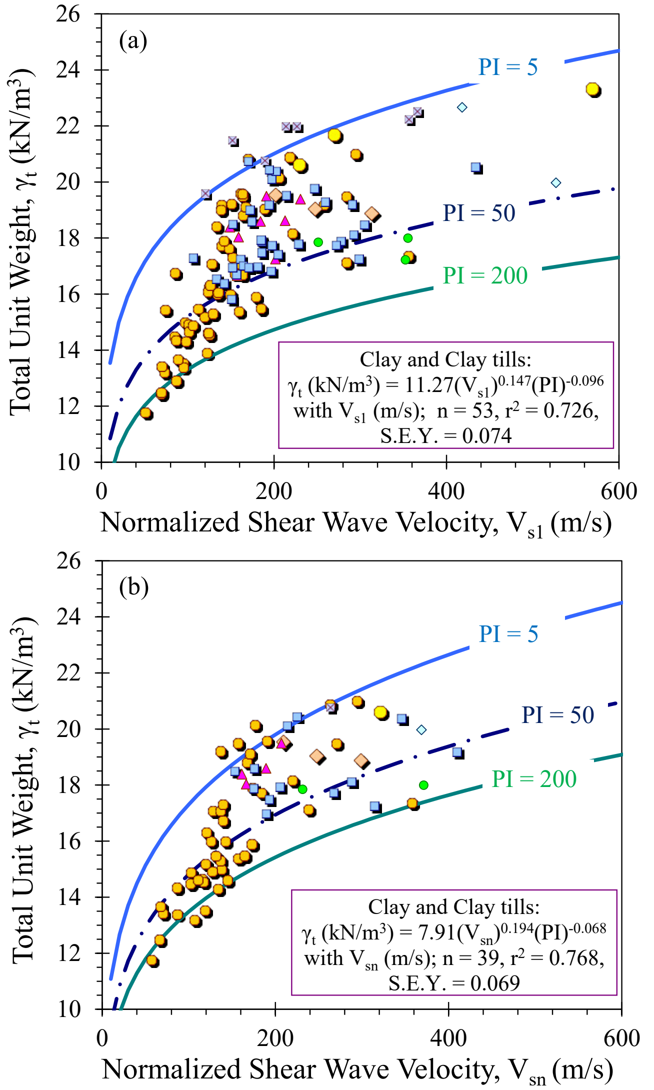

Figure 1. Total unit weight versus normalized shear wave velocity with prediction lines from multiple regression analysis: (a) V_{s1} and (b) V_{sn}.

From the proposed empirical relationships between γ_t and V_{s1} or V_{sn}, γ_t is determined with depth via following procedures: (1) determination of σ'_{v0} with depth based on assumed initial γ_t values; (2) calculation of V_{s1} and V_{sn}; (3) estimation of γ_t with depth using Equations 3 and/or 4; (4) re-calculation of σ'_{v0}

and n using γ_t with depth obtained from previous stage; (5) re-estimation of γ_t with depth using Equation 3 and/or 4; (6) iterations of stage 4 and 5 until convergence (e.g., 2-3 times). The assumed initial γ_t values in step 1 have a little effect on the results.

2.2 Shear wave velocity – undrained shear strength

A new worldwide database was compiled towards the intent of this study, including Australia, Canada, Greece, Ireland, Italy, Japan, Korea, Norway, Singapore, Taiwan, Thailand, and United States, Figure 2. It was observed that the collected clay database exhibits a wide range of overconsolidation ratios (OCR) and PIs.

In-situ V_s and/or G_0 values were collected from several geophysical tests such as cross-hole test (CHT), and down-hole type test (DHT or seismic cone penetrometer).

Figure 2. Worldwide site locations from the compiled database in this study.

On the other hand, s_u values were selected based on various in-situ tests, including field vane shear test (FV), cone penetration test (CPT), fall cone test (FCT), pressuremeter (PMT), standard penetration test (SPT), and plate load test (PLT). s_u values from different types of laboratory tests, including isotropic consolidated undrained compression (CIUC), K_0-consolidated undrained compression (CK_0UC), and unconsolidated undrained compression (UU) were also included.

$s_{u(FV)}$ values obtained from FV were used as a primary option for this study because it is generally considered to be a reference value and also correlated with other strength parameters. It should be noted that corrected $s_{u(FV)}$ values with PI (e.g., s_u multiplied by a correction factor (μ) which varies with PI) were collected for the database. For a few sites with unknown correction information, $s_{u(FV)}$ data were assumed to be corrected values. As a second option, $s_{u(TC)}$ values that were measured from laboratory CIUC or CK_0UC tests were also used for this study. In addition, some $s_{u(CPT)}$ values were compiled based on CPT at four test sites because no other reference s_u data were available.

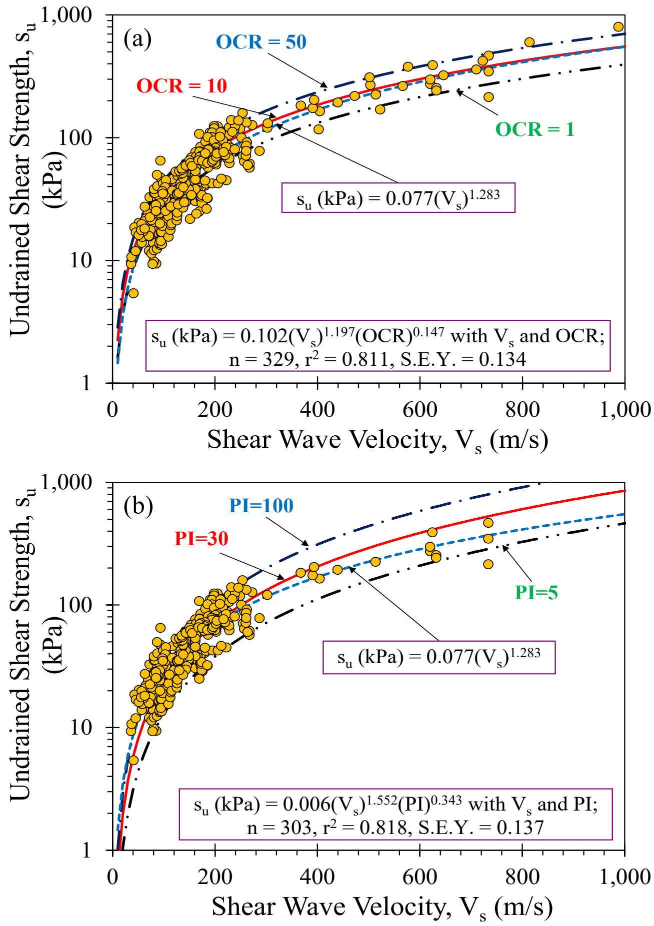

Figure 3. Trends between undrained shear strength and shear wave velocity with repect to (a) OCR, (b) PI.

Due to the dependency of the measured s_u on various factors (e.g., testing method, strain rate), it is unreasonable to compare the selected s_u values directly. Thus, several transformation methods have been proposed to convert undrained shear strength obtained from different types of tests to the reference (Bjerrum 1972; Kulhawy and Mayne 1990; Mesri and Huvaj 2007). In order to convert $s_{u(TC)}$ to the reference ($s_{u(FV)}$), this study employs a correction factor determined by comparing the ratio between $s_{u(TC)}$ and $s_{u(FV)}$. Based on the collected database, the average ratio (i.e., $s_{u(FV)}/s_{u(TC)}$=0.76) is used as the correction factor to convert the $s_{u(TC)}$ values.

Attempting to improve the fitting and statistics (e.g., R^2 and S.E.Y.), the higher order regressions are investigated by including PI or OCR with V_s in terms of s_u. Significant statistical trends relating undrained shear strength as a function of both V_s and PI or OCR are observed in Figure 3 and the multi-regressions are expressed as follows:

$$s_u = 0.102(V_s)^{1.197}(OCR)^{0.147} \quad (5)$$
$$s_u = 0.006(V_s)^{1.552}(PI)^{0.347} \quad (6)$$

3 CASE STUDIES

In order to investigate the applicability of the proposed new regression models for the estimation of γ_t and s_u, available geotechnical and geophysical data from the well-known Burswood clay in Australia and Huaiyan Expressway site in China are reviewed. These two sites were not included in each compiled database, thus independent case studies can be performed using the data from both sites.

3.1 Burswood site

Figure 4 shows the selected engineering properties of soils such as PI, OCR and V_s, based on a variety of site investigations performed for Burswood clay (Low 2009). The soil profile consisting of 3 m thick weathered crust (stiff and fine sand) and 12 m thick soft silt clay exhibits a lightly overconsolidated and sensitive silty clay, having high to uncommonly high plasticity. Shell fragments and silt lenses are frequently found in a depth of 12 m and tiny shell fragments are occasionally found at greater depth. In addtion, dessicated plants are found in a depth of 7 m (Low 2009). The profile of measured shear wave velocity is obtained from seismic cone tests, as shown in Figure 4(c).

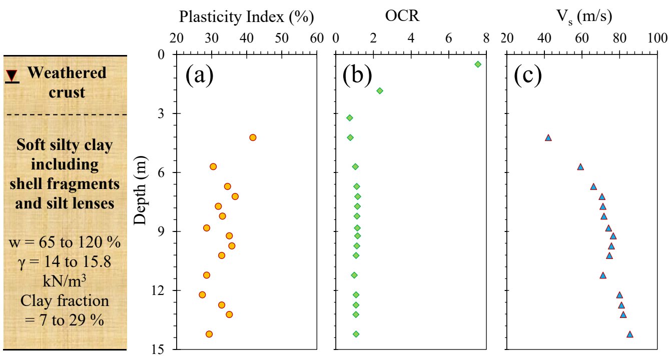

Figure 4. Case study for Burswood clay (data from Low (2009)): (a) PI, (b) OCR, and (c) V_s.

Table 2. Empirical correlations in previous studies

Empirical relationships	References
$\gamma_t\ (kN/m^3) = 30.4 \cdot PI^{0.174}$	Mayne & Peuchen (2013)
$\gamma_t\ (kN/m^3) = 6.87(V_s\ m/s)^{0.227}/(\sigma'_{v0}\ kPa)^{0.057}$	Burns & Mayne (1996)
$\gamma_t\ (kN/m^3) = 8.32\log(V_s\ m/s) - 1.61\log(z\ m)$	Mayne (2001)
$\gamma_t\ (kN/m^3) = 4.17\ln(V_{s1}\ m/s) - 4.03$	Mayne (2007a)
$\log(s_u\ (kPa)) = (\log(V_s\ (m/s)/23)/0.475$	Ashford et al. (1996)
$s_u\ (kPa) = (V_s\ (m/s)/7.93)^{1.59}$	Levesques et al. (2007b)
$s_u\ (kPa) = 0.001 \cdot V_s^{\ 2}(m/s) + 0.016 \cdot V_s\ (m/s) + 60.8$	Long et al. (2013)

Figure 5(a) compares the measured γ_t profile with the estimated γ_t profiles from the Equation 3 and 4 described in this study. In addition, the predicted γ_t profiles are compared with four empirical correlations using 1) PI from Mayne and Peuchen (2013); 2) V_s from Burns and Mayne (1996) and Mayne (2001); and 3) V_{s1} from Mayne (2007a), as listed in Table 2. As shown in Figure 5(a), γ_t of 16 kN/m³ was initially assumed. Eventually, the predicted γ_t profiles after three iterations from the equations using V_{s1} and V_{sn} derived in this study provide more reasonable agreements with the measured γ_t profile, compared with the estimated γ_t profiles from the existing correlations in previous studies.

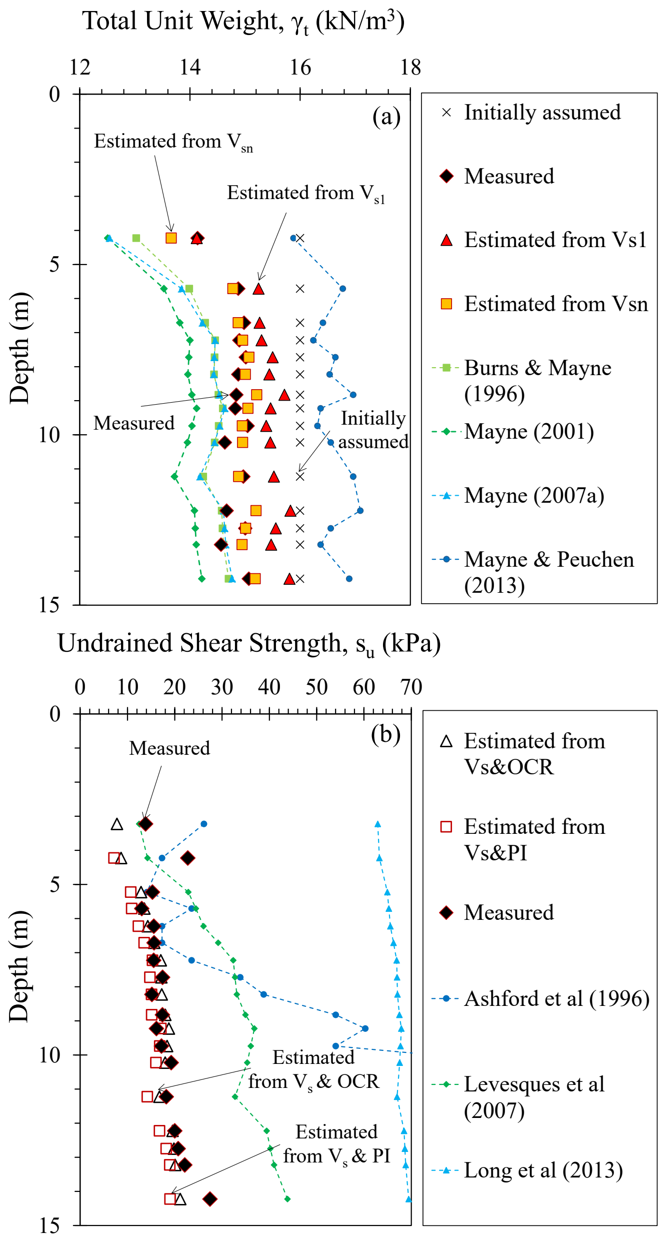

Figure 5. Comparison of estimated and measured (a) unit weight and (b) undrained shear strength at Burswood clay site.

Figure 5(b) presents the measured s_u profile from field vane shear tests, compared with the estimated s_u profiles from the Equation 5 and 6. Also, the reference s_u profile is compared with three existing empirical correlations using 1) Ashford et al. (1996); 2) Levesques et al. (2007b); and 3) Long et al. (2013), as illustrated in Table 2. Figure 5(b) shows that the predicted s_u profiles from the equations using PI and OCR derived in this study are closely matched to the measured s_u profile. Evidently, the predictions seem better matched than the other s_u profiles estimated from previous correlation studies.

3.2 *Huaiyan express site*

Huaiyan express site is located on the Lixia River area which is near the city of Yancheng in East Juangsu province, China. Figure 6 shows soil profiles determined from the geotechnical site investigations using samples from boreholes and the laboratory test results (Anand et al. 2011; Cai et al. 2015; Cai et al. 2010). The soil layers consist of a clay fill and slightly overconsolidated lacustrine clay deposit of the Holocene age. Also, the soil boundary between highly sensitive and moderately sensitive clay was found at approximate depth of 13 m. From Seismic Piezocone Test (SCPTu), it is noted that the generation of pore water pressure is remarkably increased with depth in the muck layer and dramatically decreased again (i.e., below 12 m). In addition, Figure 6(c) presents shear wave velocity measurements obtained from SCPTu.

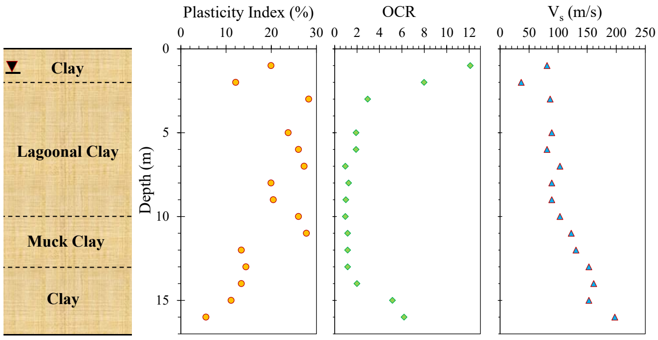

Figure 6. Case study for Hauiyan express site (data from Anand et al. (2011), Cai et al. (2015), Cai et al. (2010)): (a) PI, (b) OCR, and (c) V_s.

Figure 7(a) compares the measured γ_t profile with the estimated γ_t profiles from the Equation 3 and 4 in this study as well as other four empirical correlations. As presented in Figure 7(a), γ_t of 16 kN/m^3 was assumed in the initial stage and the evolved γ_t profiles are obtained after three iterations from the equations using V_{s1} and V_{sn} derived in this study. The final prediction profiles show more reasonable agreements with the measured γ_t profile than the estimated γ_t profiles from the existing correlations in the depth range of 3m to 12m. The underestimation of predicted γ_t at depths of below 13m can be attributed to the existence of the boundary changing from highly sensitive clay to moderate sensitive clay.

Figure 7(b) presents the measured s_u profile from field vane shear tests and the estimated s_u profiles from the Equation 5 and 6. Again, the reference s_u profile is compared with three existing empirical correlations. Figure 7(b) shows that the predicted s_u profiles from the equations using PI and OCR in this study provide relatively good agreements with the measured s_u profile.

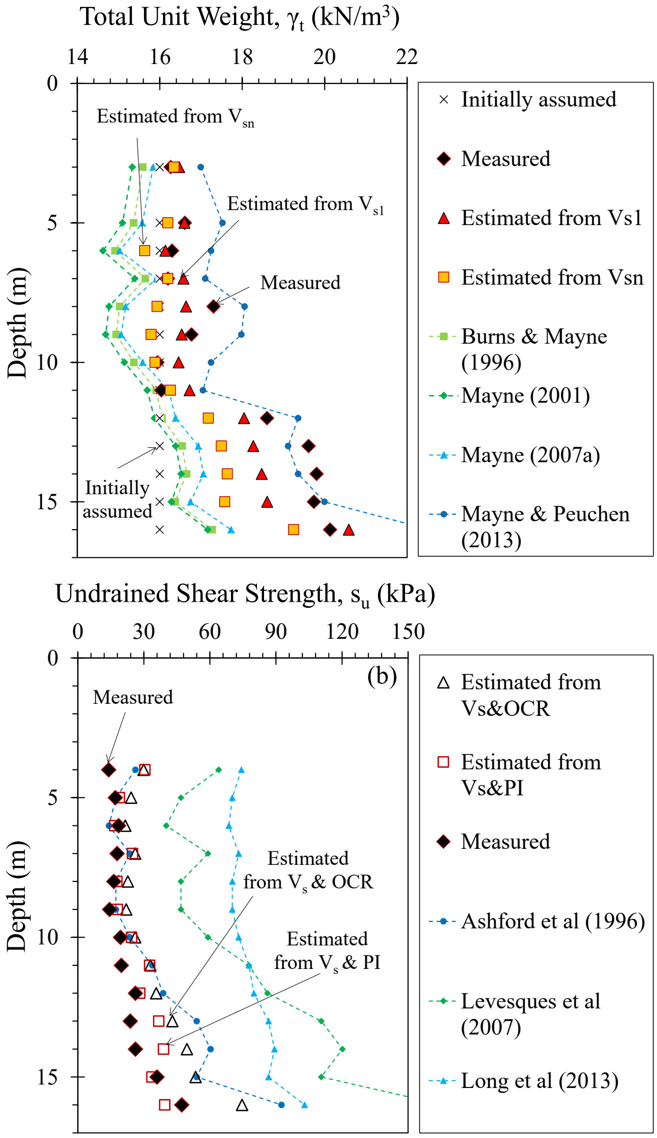

Figure 7. Comparison of estimated and measured (a) unit weight and (b) undrained shear strength at Huaiyan express site.

4 CONCLUSIONS

In this study, the global correlation models between: (1) soil unit weight and normalized shear wave velocities (V_{s1} and V_{sn}), and (2) undrained shear strength and shear wave velocity were investigated via each special database compiled worldwide. Two case studies (i.e., Burswood and Huaiyan Express) were examined for the estimation of γ_t and s_u. For estimating soil unit weight and undrained shear strength, consequently, newly developed V_s-based empirical expressions from multiple regression studies which are combined with OCR or PI are recommended beyond various previous empirical approaches.

5 REFERENCES

Anand, J.P., Guojun, C., Liyuan, T., Songyu, L., 2011. Assessment of the coefficient of lateral earth pressure at rest (K o) from in situ seismic tests. Geotechnical Testing Journal, 34(4), 1-11, doi: 10.1520/GTJ102520.

Ashford, S.A., Jakrapiyanum, W., Lukkanaprasit, P., 1996. Amplification of earthquake ground motions in Bangkok.

Bjerrum, L., 1972. Embankments on soft ground. ASCE Specialty Conference on Performance of Earth and Earth-Supported Structures. ASCE, Purdue University, Lafayette, Ind., 1-54.

Burns, S.E., Mayne, P.W., 1996. Small- and high-strain measurements of in-situ soil properties using the seismic cone penetrometer. National Academy Press, Washington, DC.

Cai, G., Liu, S., Puppala, A.J., 2015. Evaluation of geotechnical parameters of a lagoonal clay deposit in Jiangsu Lixia River area of China by seismic piezocone tests. KSCE Journal of Civil Engineering, 1-14.

Cai, G., Liu, S., Tong, L., 2010. Field evaluation of deformation characteristics of a lacustrine clay deposit using seismic piezocone tests. Engineering Geology, 116(3), 251-260.

Ghionna, V., Jamiolkowski, M., 1991. A critical appraisal of calibration chamber testing of sands. . 1st International Symposium on Calibration Chamber Testing (ISOCCTI). Elsevier, Potsdam, N.Y, 13-39.

Hight, D.W., Bond, A.J., Legge, J.D., 1992. Characterization of the Bothkennar clay : an overview. Geotechnique, 42(2), 303-347.

Kayen, R.E., Moss, R.E.S., Thompson, A.M., Seed, R.B., Cetin, K.O., Der Kiureghian, A., Tanaka, Y., Tokimatsu, K., 2013. Shear-Wave Velocity–Based Probabilistic and Deterministic Assessment of Seismic Soil Liquefaction Potential. Journal of Geotechnical and Geoenvironmental Engineering, ASCE, 139(3).

Ku, T., Mayne, P.W., 2014. Stress history profiling using OCD-G_0 anisotropy relationship. Geotechnical Engineering, Proceedings of the Institution of Civil Engineers (ICE) journal, 167(5), 476-490.

Ku, T., Mayne, P.W., Gutierrez, B.J., 2011. Hierachy of Vs modes and stress-dependency in geometerials. 5th International Symposium on Deformation Characteristics of Geometerials, Seoul, 533-540.

Kulhawy, F.H., Mayne, P.W., 1990. Manual on estimating soil properties for foundation design. Electric Power Research Inst., Palo Alto, CA (USA); Cornell Univ., Ithaca, NY (USA). Geotechnical Engineering Group.

Levesques, C.L., Locat, J., Leroueil, S., 2007a. Characterization of postglacial sediments of the Saguenay Fjord, Quebec. Characterization and Engineering Properties of Natural Soils. Taylor & Francis Group, London, 2645-2677.

Levesques, C.L., Locat, J., Leroueil, S., 2007b. Characterization of postglacial sediments of the Saguenay Fjord, Quebec. In: Tan, T.S., Phoon, K.K., HIght, D.W. & Leroueil, S. (eds.) Characterization and Engineering Properties of Natural Soils. Taylor & Francis Group, London, 2645-2677.

Long, M., Quigley, P., O'Connor, P., 2013. Undrained shear strength and stiffness of Irish glacial till from shear wave velocity. Ground Engineering, 26-27.

Low, H.E., 2009. Performance of Penetrometers in Deepwater Soft Soil Characterisation. Doctor of Philosophy, The University of Western Australia.

Mayne, P.W., 2001. Stress-strain-strength-flow parameters from seismic cone tests. Intl. Conf. on In-Situ Measurement of Soil Properties & Case Histories, Bali, Indonesia, 27-48.

Mayne, P.W., 2007a. In-situ test calibrations for evaluating soil parameters. . Characterization & Engineering Properties of Natural Soils. Taylor & Francis Group, London, 1602-1652.

Mayne, P.W., 2007b. Synthesis 368: Cone Penetration Testing. National Cooperative Highway Research Program (NCHRP).

Mayne, P.W., Peuchen, J., 2013. Unit weight trends with con resistance in soft to firm clays. Geotechnical and Geophysical Site Characterization 4. Taylor & Francis Group, London, 903-910.

Mesri, G., Huvaj, N., 2007. Shear strength mobilized in undrained failure of soft clay and silt deposits. Proceedings of Geo-Denver, 1-22.

Stokoe, K.H., Lee, S.H.H., Knox, D.P., 1985. Shear moduli under true triaxial stresses. Advances in the Art of Testing Soil Under Cyclic Conditions. ASCE Convention, Detroit.

Stokoe, K.H., Santamarina, J.C., 2000. Keynote: Seismic wave-based testing in geotechnical engineering. GeoEng 2000, Melbourne, Australia, 1490-1536.

Tatsuoka, F., Shibuya, S., 1992. Deformation characteristics of soil and rocks from field and laboratory tests, Keynote Lecture. IX Asian Conference on SMFE, Bangkok, 101-190.

Uzielli, M., Mayne, P.W., Cassidy, M.J., 2013. Probabilistic assessment of design strengths for sands from in-situ testing data. In: (series), A.i.S.M.G.-n.E. (ed.) Modern Geotechnical Design Codes of Practice. IOS-Millpress, Amsterdam, 214-227.

Yu, P., Richart, F.E., Jr., 1984. Stress ratio effects on shear modulus of dry sands. Journal of Geotechnical and Geoenvironmental Engineering, ASCE, 110(3), 331-345.